Light Detection and Ranging-Based Measures of Mixed Hardwood Forest Structure

Todd J. Hawbaker, Terje Gobakken, Adrian Lesak, Eric Trømborg, Kirk Contrucci, and Volker Radeloff

Abstract: Light detection and ranging (LiDAR) is increasingly used to map terrain and vegetation. Data collection is expensive, but costs are reduced when multiple products are derived from each mission. We examined how well low-density leaf-off LiDAR, originally flown for terrain mapping, quantified hardwood forest structure. We measured tree density, dbh, basal area, mean tree height, Lorey's mean tree height, and sawtimber and pulpwood volume at 114 field plots. Using univariate and multivariate linear regression models, we related field data to LiDAR return heights. We compared models using all LiDAR returns and only first returns. First-return univariate models explained more variability than all-return models; however, the differences were small for multivariate models. Multiple regression models had R^2 values of 65% for sawtimber and pulpwood volume, 63% for Lorey's mean tree height, 55% for mean tree height, 48% for mean dbh, 46% for basal area, and 13% for tree density. However, the standard error of the mean for predictions ranged between 1 and 4%, and this level of error is well within levels needed for broad-scale forest assessments. Our results suggest that low-density LiDAR intended for terrain mapping is valuable for broad-scale hardwood forest inventories. FOR. SCI. 56(3):313–326.

Keywords: forest inventory, pulpwood, sawtimber, timber volume, Wisconsin

QUANTIFYING FOREST STRUCTURE is essential for forest management activities such as harvest planning, habitat assessment, and ecosystem modeling. Indeed, few forest management decisions are made without forest inventory information (Avery and Burkhart 2002). Basal area, tree height, and stand-level tree volumes are among the most important measurements affecting forest plans (Næsset 1997a). Stand and canopy structure affect patterns of light transmission (Canham et al. 1994, Kucharik et al. 1999), microclimate (Chen et al. 1999), forest development (Waring 1983, Singer and Lorimer 1997), and wildlife habitat (MacArthur and MacArthur 1969). When quantified at landscape scales, forest and stand structure can inform a wide variety of management and planning activities ranging from timber harvest to biodiversity conservation.

Field-based timber inventories (or "cruises") typically measure variables such as dbh and height of trees on a number of sampling plots. These measures are summarized into variables that are relevant for timber planning at the stand scale, such as basal area and total timber volume (Avery and Burkhart 2002). Field-based inventory methods are well developed and accurate if enough plots are measured, but the main drawbacks are the time and cost required for implementing field-based inventories across broad spatial extents.

Broad-scale forest inventories have relied on manual and automatic interpretation of aerial photographs and satellite imagery (Wulder and Franklin 2003). Aerial and satellite imagery measure the spectral reflectance of the canopy and have been successfully used to map crown perimeters (Brandtberg and Walter 1998), species composition (Wolter et al. 1995), stand boundaries (Leckie et al. 2003b), burned areas (Jakubauskas et al. 1990), and insect defoliation (Radeloff et al. 1999). However, despite the wealth of information that can be produced from imagery of canopy reflectance, it remains difficult to derive information about forest attributes that are most relevant for forest managers, such as stem density, dbh, basal area, tree height, and volume (Hudak et al. 2002, McCombs et al. 2003).

Light detection and ranging (LiDAR) generates three-dimensional data that are capable of mapping forest attributes (Nelson et al. 1984, 1988, Nilsson 1996, Næsset 1997b, Lefsky et al. 1999). LiDAR sensors are typically mounted in an aircraft, and the exact location of the sensor is measured using differential global positioning systems (GPS) plus an inertial navigation system that controls for the aircraft's

Todd J. Hawbaker, University of Wisconsin, Forest and Wildlife Ecology, 1630 Linden Drive, Madison, WI 53706—Phone: (608) 469-7907; Fax: (608) 262-9922; tjhawbaker@gmail.com; Current address: US Geological Survey, Rocky Mountain Geographic Science Center, Denver, CO. Terje Gobakken, Norwegian University of Life Sciences—terje.gobakken@umb.no. Adrian Lesak, University of Wisconsin—lesak@wisc.edu. Eric Trømborg, Norwegian University of Life Sciences—erik.tromborg@umb.no. Kirk Contrucci, Ayers Associates, Inc.—contruccik@ayresassociates.com. Volker Radeloff, University of Wisconsin—radeloff@wisc.edu.

Acknowledgments: We are most grateful for support for this study by the Wisconsin Department of Natural Resources, the US Forest Service Northern Research Station, and the US Department of Agriculture McIntire-Stennis Program. The Wisconsin Department of Natural Resources funded collection of field data, and Ayres Associates and Sauk County generously provided the LiDAR data and digital elevation models used in this research. All fieldwork was conducted on property managed by the Wisconsin Chapter of The Nature Conservancy and the Wisconsin Department of Natural Resources and we appreciate permission to work on their land. GPS units were provided by University of Wisconsin Kemp Natural Resources Station and David Mladenoff's Forest Landscape Ecology Laboratory at University of Wisconsin–Madison. Mathew Duffy, Jason Jones, Terry Kocsis, Joseph Nadolski, and Paul Schilke, were a tremendous help in collecting data in the field. We also thank three anonymous reviewers and Jordan Muss for providing critical comments that improved the article.

Manuscript received February 25, 2008, accepted November 11, 2009

heading, pitch, roll, and yaw. There are two general types of LiDAR systems: waveform and discrete (Lefsky et al. 2002, Lim et al. 2003).

Waveform LiDAR collects continuous data that records the vertical profile of reflected laser energy from vegetation and the ground over relatively large footprints (>1 m) (Nilsson 1996, Lefsky et al. 1999). All past, existing, and planned space-borne LiDAR platforms collect waveform data (Shuttle Laser Altimeter [SLA], Gavin et al. 1998; Vegetation Canopy LiDAR [VCL], Dubayah et al. 1997; Ice, Cloud, and Land Elevation Satellite [ICESat], Harding and Carabajal 2005, and Deformation, Ecosystem Structure, and Dynamics of Ice [DESEynI], Donnellan et al. 2008), although airborne waveform sensors also exist, such as SLICER (Blair et al. 1994, Harding et al. 1994) and Laser Vegetation Imaging Sensor (LVIS) (Blair et al. 1999).

In contrast with waveform systems, discrete LiDAR sensors measure the distances between an infrared laser-emitting sensor and target objects by calculating the difference in time between emission of a laser pulse and the return of a portion of the pulse reflected off objects; typically between 1 and 5 returns are recorded (Baltsavias 1999a). Discrete return LiDAR is preferred for elevation mapping because the small pulse footprints (<1 m) are more capable of penetrating vegetation canopies to measure ground elevations. The high resolution and density of discrete LiDAR sensors also make their data suitable for object detection, such as individual trees (Brandtberg et al. 2003) or buildings (Haala and Brenner 1999, Maas and Vosselman 1999). Discrete LiDAR platforms are common in private industry and are deployed via helicopters or fixed-winged aircraft (Baltsavias 1999b).

In forests, the first return from discrete LiDAR is usually reflected off leaves and branches in the canopy, whereas subsequent returns are reflected off lower leaves and branches or the ground. Returns above the ground or returns classified as vegetation are used to construct canopy surface models, and the basic idea behind LiDAR-based forest inventories is that the volume of space under the canopy surface is directly related to total biomass and hence timber volume. Spatial variability in canopy volume is reflected in the number of returns penetrating the canopy surface and reflecting off of lower branches, leaves, and the ground, and these differences can be estimated using a variety of metrics summarizing the vertical distribution of LiDAR vegetation returns.

LiDAR data have been used to describe forest structure using two general approaches relating to the scale of analysis; single tree identification and data aggregation. Single-tree approaches, using discrete LiDAR data, identify individual trees and characterize their height, canopy structure, volume, and other characteristics (Brandtberg et al. 2003, Leckie et al. 2003a). When high-density LiDAR data are available, the single-tree approach might be desirable because it corresponds directly to the smallest observable object in timber inventories: the tree (Hyyppä et al. 2001). However, single-tree approaches are difficult to implement across large areas, because they are data-intensive and provide limited information about subdominant trees, depending on canopy density (Maltamo et al. 2005, 2007 Takahashi et al. 2005).

An alternative to single-tree identification is LiDAR data aggregation, when both LiDAR returns and vegetation information are collected over some larger spatial footprint. By design, waveform LiDAR data integrate reflectance through vertical space within each footprint. When discrete LiDAR pulses or pulse intensities are aggregated at a different spatial scale, they emulate the waveform LiDAR (Blair and Hofton 1999). This approach with discrete LiDAR data is flexible because the data can be summarized within fixed-area units, such as pixels (Nelson et al. 1988) but also irregularly shaped segments (van Aardt et al. 2006) or forest stands (Næsset 1997b). Aggregation also has the practical benefit of reducing the volume of discrete LiDAR returns to more manageable grids or polygons, while maintaining the information relevant for vegetation measurement. Operationally, this process allows for timber attributes to be rapidly derived from LiDAR data over large areas with minimal processing effort (Næsset 2004, Næsset et al. 2004).

Increasingly, discrete LiDAR data are being collected for a diverse range of applications including timber inventory (Næsset et al. 2004), fuel load estimation (Riano et al. 2003), vegetation and habitat mapping (Hinsley et al. 2002, Hill and Thomson 2005), and generation of terrain and hydrology models (Bufton et al. 1991, Lohr 1998, Cobby et al. 2001). Collection of LiDAR data can be expensive, but costs per product decrease if multiple products can be derived from the same LiDAR data. Hence, there remains a need to determine whether LiDAR data not originally intended for vegetation mapping are suitable for forestry applications.

Elevation mapping is possible with low-density LiDAR data collected during leaf-off when conditions are ideal for pulses reaching the ground (Anderson et al. 2005). Previous studies have demonstrated the potential use of LiDAR for inventories of coniferous and hardwood forests (Lim et al. 2003, Holmgren 2004, Næsset 2004), even with relatively low pulse densities up to 0.06 pulse/m^2 (Magnusson et al. 2007, Gobakken and Næsset 2008). However, LiDAR data for forestry applications are typically collected in leaf-on conditions when most pulses are reflected from canopy vegetation, and the physical model of LiDAR reflections in leaf-off canopies differs substantially from that in leaf-on canopies. In the physical model for leaf-on canopies, the shape of the crown determines the vertical distribution of the majority of the plant material that intercepts LiDAR pulses and hence the LiDAR waveform (Sun and Ranson 2000). Vegetation clumping, such as leaves clustering into tree crowns, affects the waveforms, and higher clumping will result in less returns from the canopy than would be expected for horizontally homogeneous plant canopies (Ni-Meister et al. 2001).

The physical model for LiDAR reflections under leaf-off conditions is rather different though, because only the branches of trees can intercept LiDAR pulses. This means that a higher proportion of LiDAR pulses will reach the ground (Anderson et al. 2005), and less information about the vegetation is provided (Brandtberg et al. 2003), which

will affect in particular LiDAR metrics that incorporate last returns (Brandtberg et al. 2003, Næsset 2005, Brandtberg 2007). The different physical model also means that LiDAR first returns will occur lower in the canopy, than is the case for leaf-on LiDAR potentially limiting the ability to estimate total height accurately.

However, this difference in the physical model suggests that leaf-off LiDAR may have benefits over leaf-on LiDAR when it comes to estimating merchantable height and hence merchantable volume. In hardwood trees, merchantable height is greatly affected by the branching structure, especially when sawlog volume is estimated, for which the requirement for a minimum diameter inside bark is more stringent than for pulpwood volume (Avery and Burkhart 2002). If we assume that two trees have the same total height, then merchantable volume will be much higher for a tree with branches only high up in the canopy compared with that for a tree that branches out low on the trunk. Given the physical model, the tree with lower branches would exhibit substantially lower LiDAR returns than the tree with only canopy branches. The physical model thus suggests that leaf-off LiDAR may have an advantage over leaf-on LiDAR when it comes to the estimation of merchantable height in hardwood trees, whereas leaf-on LiDAR would probably perform better in terms of total height measurements. However, the ability of leaf-off LiDAR to predict tree attributes and in particular merchantable volume has not been fully explored.

Our primary goal was to determine how well low-density LiDAR collected in leaf-off conditions can inventory the uneven-aged, mixed hardwood forests that are typical for large portions of eastern North America. Furthermore, we were interested in how sensitive our results were to which LiDAR returns were used (i.e., first or canopy returns compared with ground returns). The three specific questions we sought to answer were the following: How well do univariate models using aggregated LiDAR data explain field-measured timber attributes in the mixed hardwood forests of southern Wisconsin? Do multivariate regression models with several LiDAR variables increase the amount of variability explained? Do model fits change when different types of LiDAR returns are used (first returns only versus all returns)?

Methods

Study Area

Southern Wisconsin is an ideal location for LiDAR-based forest inventories because of the state's extensive forested areas, the diversity of forest types, and the importance of accurate, broad-scale forest inventories for many forest stakeholders. Our study area was located in the Baraboo Hills in Sauk County, part of the Driftless Region of southwestern Wisconsin (89.850°W, 43.385°N to 89.640°W, 43.391°N). Designated a National Natural Landmark in 1979, the Baraboo Hills are prized for their large blocks of contiguous forest and for their diversity of natural communities, including the largest intact southern upland forest in the prairie-forest border ecoregion. Most forests in this region were cleared by the 1870s. Since then, 140 years of high grading, mixed with some clear cutting, agricultural abandonment, and passive management has made the forest mixed in age. Currently, upland forests are dominated by oak (*Quercus* spp.), ash (*Fraxinus* spp.), and hickories (*Carya* spp.) with sugar maple (*Acer saccharum*), red maple (*Acer* rubrum), and basswood (*Tilia americana*) as common associates. Remnant white pine (*Pinus strobus*), hemlock (*Tsuga canadensis*), and yellow birch (*Betula alleghaniensis*) stands are present on cooler north facing slopes.

We sampled 114 plots located within Devil's Lake State Park and The Nature Conservancy's Baxter's Hollow Preserve. The total area of these two parcels is approximately 6,000 ha (14,800 acres), of which 4,580 ha (11,300 acres) is forested. Field plots were arranged in a systematic design. Plots were arranged along parallel transects; we used 600 m (1,969 ft) spacing between transects and 300 m (984 ft) between plots in each transect. We excluded sampling to forests with at least 150 m (492 ft) distance from all roads and edges.

Field Methods for Timber Inventory

We used circular, fixed-area plots with a 15.25 m (50 ft) radius. We chose this radius to ensure that at least 100 LiDAR returns would fall within the plot boundaries. The location of each plot center was mapped with submeter accuracy using postprocessed differentially corrected GPS data collected with a Trimble ProXRS unit. Differential correction was performed with data from the Madison, WI, City Engineering Department's Continuously Operating Reference Stations, approximately 45 km (30 miles) from the study area. On average, 215 GPS positions were collected at each plot and postprocessed horizontal precision was 0.57 m (1.9 ft).

Within the fixed-area plot, we recorded dbh, tree species, and status (live or dead) and whether or not the tree had excessive lean for all trees with dbh $\geq$12.7 cm (5 in.). Using a prism with a 2.3 m^2/ha (10 ft^2/acre) basal area factor, a subset of these trees was selected for total height measurement with a Haglöf Vertex III Hypsometer. On average, there were 31.1 trees per plot and height was measured for 9.6 trees per plot. This left many trees without height measurements. For these trees, we predicted total height using regression models with the form ln(height) = ln(dbh) for height predictions (Avery and Burkhart 2002). We chose this model form over more complicated height models because we had no additional information about variables that might influence tree height, such as site index (Ek et al. 1981). Instead, we chose to account for plot-level differences in the relationship between height and dbh by allowing the intercept and slopes to vary among plots. The model was fit as a linear mixed-effects model in R using the nlme library (Pinherio and Bates 2002).

We used the US Forest Service National Volume Estimator Library (NVEL) to estimate the total merchantable sawtimber and pulpwood volume for each tree (US Forest Service 2006). For the Great Lakes region, the NVEL library generates volume estimates based on dbh and total height (Gevorkiantz and Olsen 1955). Tree volumes (excluding bark) were calculated for all trees with dbh $\geq$12.7

cm (5 in.), assuming a 30.5-cm (1-ft) stump. Volume estimates were made using equations developed for National Forests in Wisconsin. For this region, the NVEL library calculates sawtimber volumes using the Scribner Decimal C rule in board feet units and pulpwood volumes as cords. We converted pulpwood volumes in cords to m^3 with a 3.6 (m^3/cord) conversion factor (Avery and Burkhart 2002). We converted board feet volumes to cubic meter volumes, assuming that 1,000 bd ft using the Scribner Decimal C rule were equivalent to 5.4 and 4.9 m^3 of solid wood for softwood and hardwood species, respectively. These conversion factors were based on Wisconsin averages (Tom Steele, pers. comm., Kemp Natural Resources Station, University of Wisconsin, Dec. 4, 2007) and assumed that 1,000 bd ft was equivalent to 2.4 (softwoods) and 2.2 (hardwoods) cords. We also assumed that each cord of stacked wood occupied 3.6 m^3 and that 61.7% of a cord was solid wood.

Finally, we generated plot-level summaries of the individual tree measurements including tree density, mean dbh, basal area, mean tree height, Lorey's mean height (basal area weighted tree height), and sawtimber and pulpwood volumes (Table 1). These plot-level summary variables were then used as response variables in regression models with LiDAR summary variables as the predictors.

LiDAR Sensor

LiDAR data were collected using a Leica ALS50 airborne laser scanner flown in leaf-off conditions during May 2005 with an altitude of 1,981 m (6,500 ft) and flight speed of 241 km/h. LiDAR pulse frequency was 34,700 Hz, and the beam footprint was 68.9 cm (2.26 ft). The horizontal accuracy of pulses was estimated to be 0.5 m. The vertical accuracy was estimated at 15 cm root mean square error (RMSE) using known benchmark elevations from a countywide surveying network.

LiDAR Processing and Summary

We constructed a digital elevation model (DEM) with 5 m (16.4 ft) resolution from the raw LiDAR data. Individual LiDAR returns were attributed with horizontal coordinates as well as an elevation. For each LiDAR return, height above ground was calculated by subtracting the DEM elevation from the return elevation. We assumed slope effects would be negligible within the 5-m DEM pixels.

For each field plot, the LiDAR returns within 15.25 m (50 ft) of the plot center were selected, and their heights were summarized following the methodology suggested by Næsset (2002). We developed two different LiDAR data sets. The first data set included all returns; the data contained no more than 3 returns/pulse. The second data set included only first returns, which we assumed were canopy hits. From here on, we refer to these data sets as "all-return LiDAR data" and "first-return LiDAR data." In both data sets, we considered returns with heights less than 0.9 m (3 ft) to be ground noise and excluded them from the analysis. The summary statistics we calculated include total number of returns (n), mean (mean), coefficient of variation (cv), and 10% percentiles of height aboveground (h00, h10, h20, h30, …, h80, h90, h100), and the density of returns contained within equally spaced height divisions between 0.9 m (3 ft) and the maximum height value (d10, d20, d30, …, d80, d90, d100) (Figure 1). All LiDAR predictor variables were natural log-transformed to ensure normal distribution.

Regression Modeling

Our main research goal was to determine how well the LiDAR variables could capture forest inventory variables as measured on the ground. Univariate regression models were used to identify general relationships and to help understand which LiDAR variables are most related to the field data. We also constructed multivariate linear regression models to determine how much variance in the field data can be explained by combinations of LiDAR variables. Many of our LiDAR summary variables were highly correlated. Before constructing multivariate regression models, we examined the correlations among the transformed variables and constructed a list of all potential models that had at least 3 variables with $<50\%$ correlation among them. This resulted in 212 multiple linear regressions models for the all-return data and 222 potential models for the first-return data. We chose this approach over stepwise selection because variable selection can be confounded by highly correlated predictor variables. We selected the top three models that explained the most variability in the data, based on adjusted R^2 values. These three models were subjected to more rigorous evaluation of linear regression assumptions (linear relationship, constant variance, and random errors). All statistical analyses were conducted with R version 2.4.1 (R Development Core Team 2007).

During regression modeling, observations from one plot were found to be an outlier and we removed it from the sample. This particular plot had only a few small-diameter trees with basal area of 2.1 m^2/ha (9 ft^2/acre) and no sawtimber or pulpwood volume. Even though this plot was a valid observation we removed it from the sample because

Table 1. Response variables summarized from field-base timber inventory and range of observed values

	Tree density (trees/ha)	Mean dbh (cm)	Basal area (m^2/ha)	Mean tree height (m)	Lorey's mean tree height (m)	Sawtimber volume (m^3/ha)	Pulpwood volume (m^3/ha)
Minimum	169.8	18.4	10.0	13.0	14.3	4.8	112.9
25% quartile	328.9	25.5	23.5	17.5	19.4	82.9	287.4
50% quartile	382.0	27.9	28.9	19.2	21.2	130.8	351.3
Mean	408.0	28.4	29.1	19.4	21.3	140.0	366.1
75% quartile	481.0	31.2	34.0	21.0	23.3	189.3	441.2
Maximum	749.8	41.1	53.3	26.8	28.8	408.0	779.8

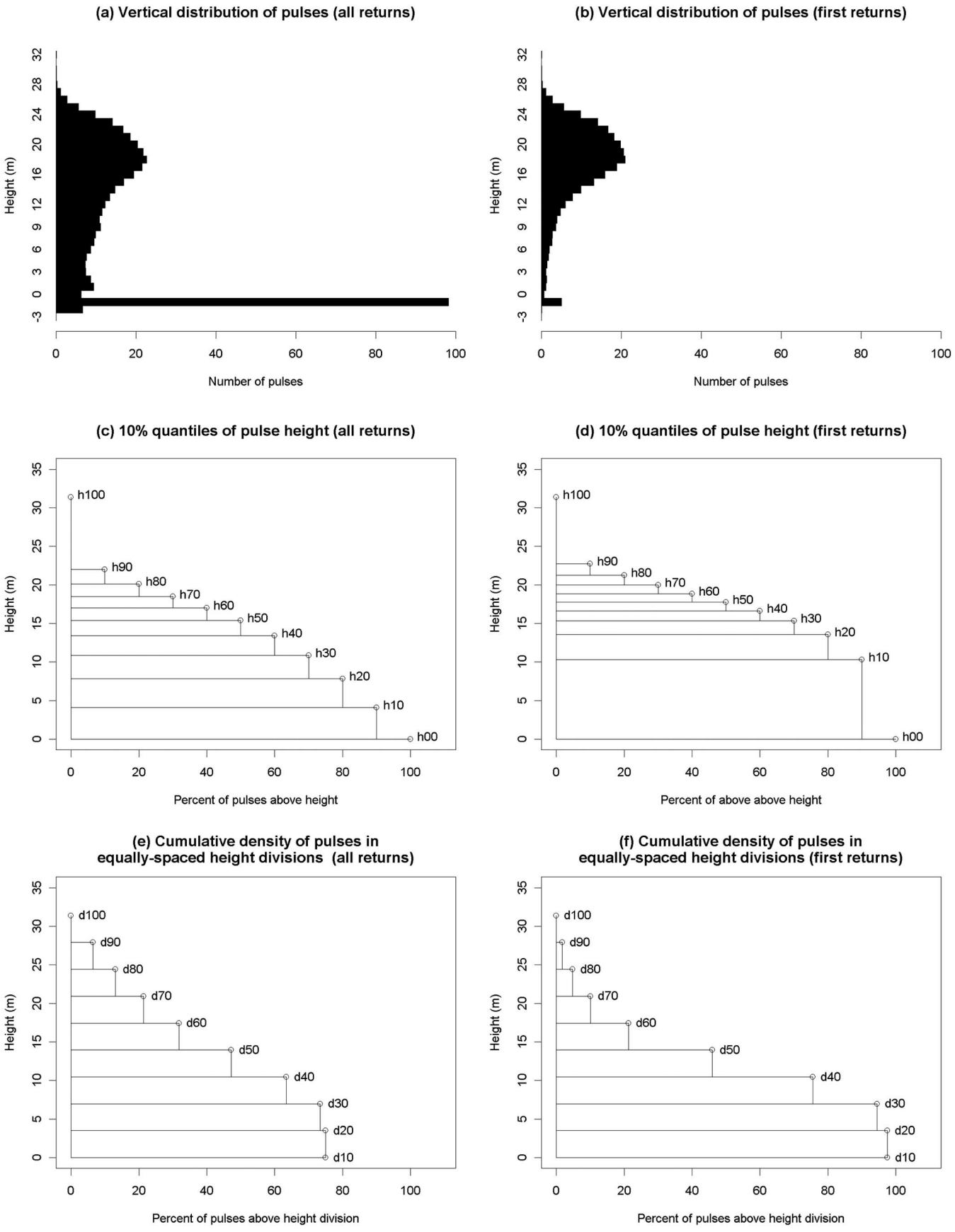

Figure 1. Histograms of the vertical distribution of pulse heights for (a) all returns and (b) first returns only, 10% height quantiles with variable names in regression analysis for (c) all returns and (d) first returns only, and cumulative density of pulses in equally spaced height divisions for (e) all returns and (f) first returns only. All graphs were generating using pulses heights averaged across all field plots.

it clearly fell beyond the range of variability observed in the remainder of the sample.

Regression Model Cross-Validation

We evaluated the predictive power of our final group of multivariate regression models using a leave-one-out cross-validation strategy (Stone 1974, Efron 1982). We chose a leave-one-out cross-validation strategy over other validation methods that use larger data subsets for validation for several of reasons. First, other than rules of thumb, there is little guidance to determine the size of sample to use for validation. Second, the resulting errors are consistently overestimated and are largely dependent on the number of observations in the training and validation (Olden and Jackson 2000). The cross-validation strategy we implemented excluded one observation and constructed models using the remaining $n - 1$ observations. The resulting model was used to make predictions for the excluded observation. Error was calculated based on the difference between the predicted and observed values for the excluded observation. This procedure was repeated 114 times, so that prediction errors were calculated for each observation in the data set. This method generally produces unbiased estimates of prediction errors (Olden and Jackson 2000). We then calculated the range, mean, and SD of the difference between cross-validated predictions and original observations. Differences were calculated after the predictions were transformed back to their original scale.

Results

Univariate models relating all-return LiDAR data summary variables to field-collected timber attributes explained a substantial proportion of the variability in the data; $R^2 =$ 62% for sawtimber volume, 61% for Lorey's mean tree height, 59% for pulpwood volume, 52% for mean tree height, 43% for mean dbh, 35% for basal area, but only 9% for tree density. For all of the univariate models except tree density, the upper height percentiles of the LiDAR variables tended to be the best predictors (Figures 2 and 3).

Regression models constructed with first-return LiDAR data summaries generally increased the amount of the variance explained and reduced cross-validated errors more than the models based on all-return LiDAR data (Figure 2). The increase in explanatory power was most notable for models of basal area. With the first-return data, the LiDAR height summary variables tended to be the most correlated with the field data, but the best model fits were produced by slightly lower height quantiles than in the all-return models.

Among the all-return and first-return univariate regression models, cross-validation RMSEs were greatest for sawtimber and pulpwood volumes. For example, the best sawtimber volume model derived from the first-return data had an R^2 of 63%, but the cross-validated RMSE was 58.61 m^3/ha (Figure 3); this was quite large considering that the average observed sawtimber volume was 140 m^3/ha across all plots (Figure 3). Errors were less for height and dbh-related measures, and cross-validated RMSE was 1.89 m for the best mean tree height model and 3.36 cm for the best model of mean dbh (Figure 3).

Compared with the univariate models, multivariate regression models constructed using the all-return LiDAR data increased the amount of variance explained for dbh, basal area, and pulpwood volume (Figure 2; Table 2). Inclusion of additional variables had the greatest effect for the model of basal area, increasing R^2 values by an additional 5, 6, and 11% over the best univariate models for mean dbh, pulpwood volume, and basal area, respectively. Models of mean tree height and sawtimber volume were slightly improved by including more variables, but the additional amount of variability that was explained was only 3%. For tree density, there were no multivariate regression models that explained additional variability over the univariate models. Among all the multivariate models, the additional variables added included coefficient of variation and the lower height quantiles and return densities.

Multivariate regressions constructed with first-return data explained little to no additional variability compared with the univariate models. The greatest gains were for tree density, mean dbh, and basal area (5, 2, and 2% increases in R^2, respectively). Compared with the all-return multivariate models, the first-return multivariate models did not explain any additional variability (Table 3), except for tree density, for which the R^2 values were 13 and 9% for the best first-return and all-return models, respectively.

Regression models can be constructed with two different goals: to identify factors that explain the most variability in observed data or to make predictions with small errors. For this study, our goal was primarily to build models of forest structure for predictive use. Thus, our results should be judged more by the errors in the predictions than by the R^2 values of individual regressions, because R^2 values for different models using different data are not necessarily comparable. All data in our models were logarithmically transformed, and errors are asymmetric when converted back to the original scale. Thus, there is a tendency to slightly underpredict values on average (Tables 2 and 3).

Discussion

Our results demonstrated that low-density LiDAR data can be used to monitor structural attributes of mixed-species hardwood forests. In general, our LiDAR models explained the most variability in sawtimber and pulpwood volumes and tree heights. However, our models also predicted average dbh and basal area reasonably well. Tree densities were most difficult to predict. Our prediction errors tended to be larger than those of previous LiDAR timber inventory studies in mature Canadian hardwood and Norwegian coniferous forests, which used greater pulse densities (Næsset 2002, Lim et al. 2003, Popescu et al. 2004). However, although our prediction errors for individual plots may have been relatively high (9% for Lorey's tree height to 40% for sawtimber volume), the standard errors of the means were within 1 to 4%. This level of error is what would be expected if our data were aggregated to the stand-level and certainly within the acceptable range of errors for forest

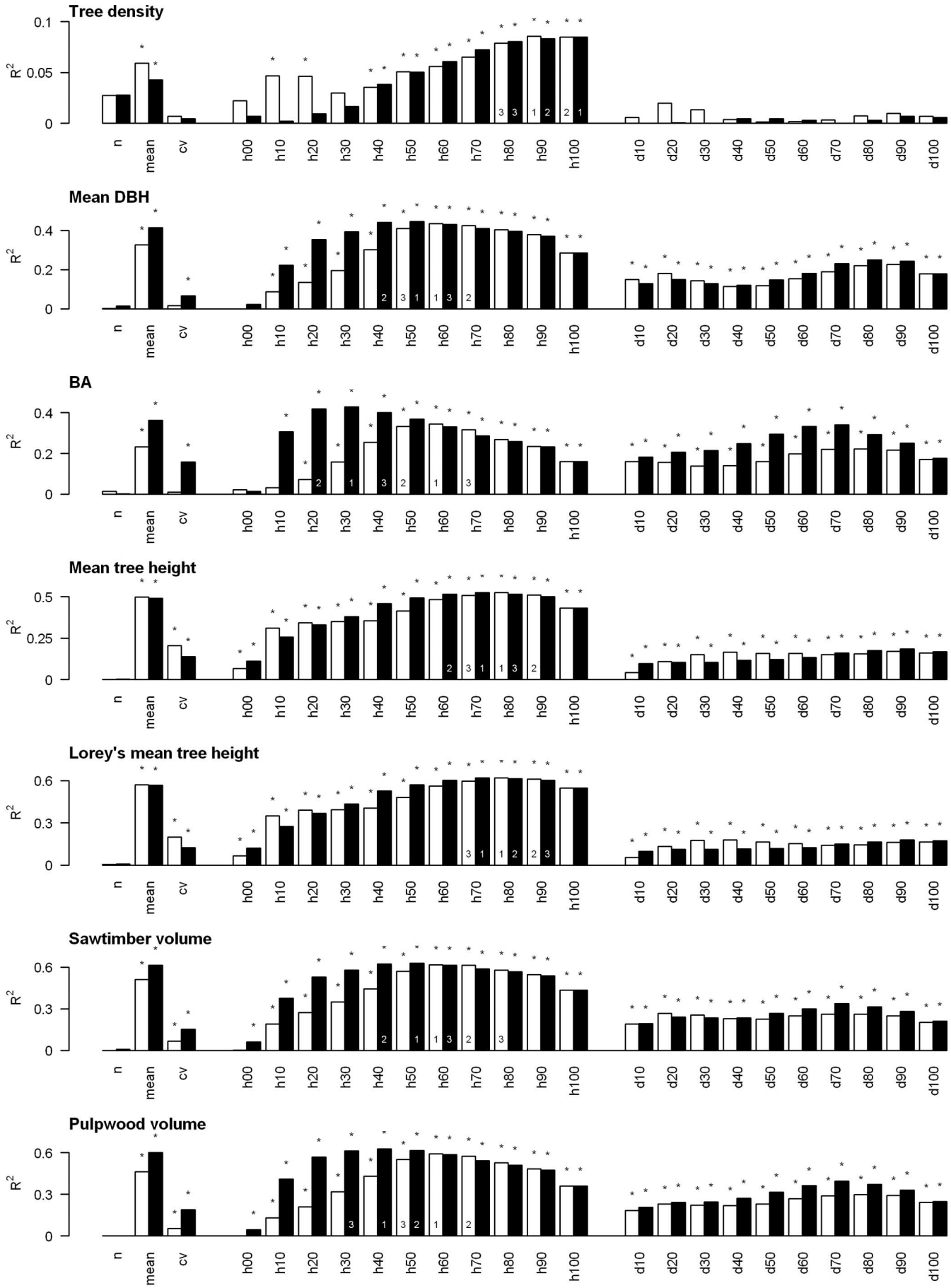

Figure 2. Univariate regression model R^2 values for all-return models (□) and first-return models (■). Asterisks above bars indicate models that were significant with $P \leq 0.05$. The top three models are indicated by numbers within the bars.

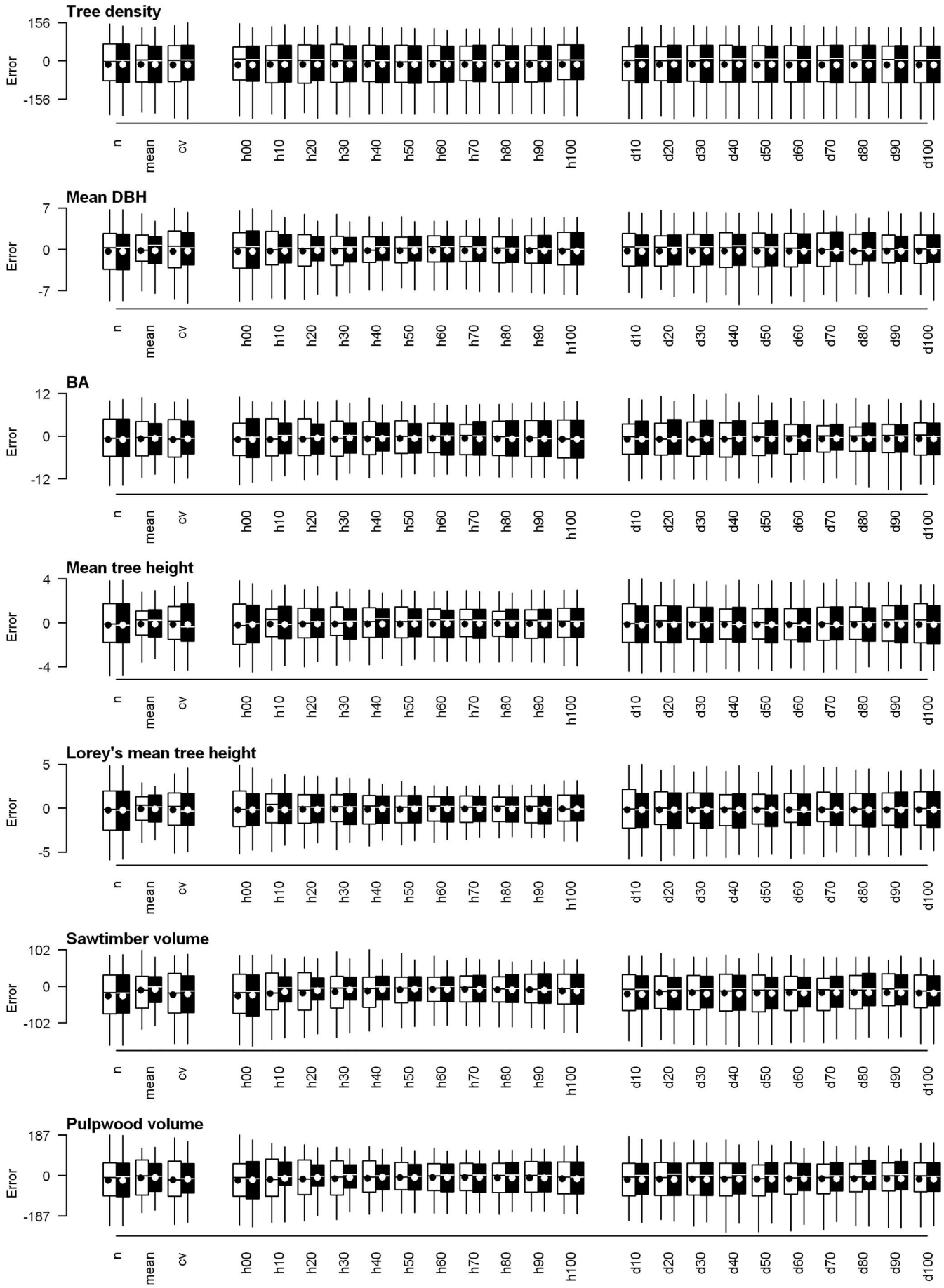

Figure 3. Univariate regression model leave-one-out cross-validation error distributions for all-return models (□) and first-return models (■). Boxes indicate 25 and 75% error quantiles. Vertical lines extending above and below boxes indicate 5 and 95% error quantiles. Horizontal lines within boxes indicate median error. Dots within boxes indicate mean error.

Table 2. Top three regression models from 212 potential models with uncorrelated predictor variables for all-return LiDAR data

Model form	R^2	Error (predicted − observed)		
		Range	Mean	SD
Tree density				
ln(h90)	0.09	−355.4−314.8	−13.9	111.5
ln(h100)	0.08	−348.2−261.8	−14.0	111.5
ln(h80)	0.08	−356.5−322.3	−14.0	111.8
Mean dbh				
ln(cv) + ln(d90) + ln(h100)	0.48	−10.2−6.48	−0.2	3.3
ln(cv) + ln(d90) + ln(h90)	0.48	−10.2−6.63	−0.2	3.3
ln(d10) + ln(h00) + ln(h70)	0.47	−10.4−6.81	−0.2	3.4
Basal area				
ln(d10) + ln(h00) + ln(h60)	0.46	−16.8−13.4	−0.5	6.0
ln(d10) + ln(h00) + ln(h50)	0.46	−16.2−14.1	−0.5	5.9
ln(d10) + ln(h00) + ln(h70)	0.43	−17.1−12.7	−0.5	6.1
Mean tree height				
ln(cv) + ln(n) + ln(h90)	0.55	−5.5−4.1	−0.1	1.9
ln(cv) + ln(h80)	0.54	−5.2−4.3	−0.1	1.9
ln(h00) + ln(h80)	0.54	−4.5−5.0	−0.1	1.9
Lorey's mean tree height				
ln(d100) + ln(h10) + ln(h100)	0.63	−4.7−5.0	−0.1	2.0
ln(cv) + ln(h90)	0.62	−4.4−5.1	−0.1	1.9
ln(d90) + ln(h10) + ln(h100)	0.62	−4.8−5.6	−0.1	2.0
Sawtimber volume				
ln(d10) + ln(h00) + ln(h60)	0.65	−156.6−119.5	−7.0	55.6
ln(d10) + ln(h00) + ln(h70)	0.64	−165.8−121.7	−6.9	56.1
ln(d10) + ln(h70)	0.63	−170.4−183.8	−7.6	59.2
Pulpwood volume				
ln(d10) + ln(h00) + ln(h60)	0.65	−214.7−173.0	−7.4	84.9
ln(h00) + ln(h60)	0.63	−244.5−189.5	−7.7	86.2
ln(d10) + ln(h00) + ln(h70)	0.63	−222.1−161.6	−7.7	86.1

Refer to the Methods for interpretation of predictor variable names. Data were transformed to original units before the differences between predicted and observed values were calculated.

inventories (Avery and Burkhart 2002) The ability of low-density LiDAR to quantify hardwood forest structure is especially encouraging because the LiDAR data we used were originally intended for constructing elevation models. Our findings support the growing body of literature, suggesting that high-density LiDAR sampling may not be necessary for broad-scale forest inventories (Magnusson et al. 2007, Gobakken and Næsset 2008).

To determine tree volumes, we used NVEL, which includes Lakes States specific equations for estimating stem volume from dbh and height (Gevorkiantz and Olsen 1955). Measured errors in volume for Red Oak in southern Wisconsin were as high as 23% for individual trees; however, when trees were aggregated to stands, individual tree errors cancel each other out and total error for volume was near 1% (Gevorkiantz and Olsen 1955).

LiDAR sensors excel at measuring object heights, and it was not surprising that our predictions of mean tree height and Lorey's mean tree height were good. We were able to predict mean height and Lorey's mean tree height with SD <2 m. In our analyses, there were several potential sources for error in height measurements. We made field measurements of heights for a subsample of trees and then predicted heights for the remaining trees. Field measures of tree height can contain substantial errors and one study found that repeated height measurements of several trees using the Vertex III Hypsometer had SDs ranging from 0.05 to 0.20 m (0.2–0.7 ft) and were consistently 1.2 m (4 ft) greater than tree heights measured using a total station (Wing et al. 2004). In addition, the residual SE of the regression model we used to predict tree height was 36.6 cm (1.2 ft). In consideration of these two sources of field measurement error, the LiDAR-based estimates of tree height performed quite well and were also near the error range of previous studies that used greater pulse densities or single-tree methods (Næsset 2002, Brandtberg et al. 2003, Lim et al. 2003, Popescu et al. 2004).

Less variance was explained by nonheight timber measurements, but cross-validated prediction errors were impressive. The average difference between our predicted and observed values was <0.2 cm for mean dbh and approximately 0.5 m^2/ha for basal area. At the scale of our analysis, we expect that these errors are well within the level of precision needed for most forestry applications. Previous studies showed that tree density or stem counts were difficult to predict (Lim et al. 2003, Næsset 2004, Popescu et al. 2004), and our study had similar problems predicting tree density. Overall, the range of prediction errors for stem density was just slightly less than the mean observed stem density; such high errors would preclude the use of LiDAR to estimate stem density.

Our results and those of previous studies provide evidence that low pulse density LiDAR data, which are widely available, can be used for forest inventories over large spatial areas. In addition to highly variable forest structure, several other factors could have influenced our results. In deciduous forests, LiDAR height measurements are dependent on the seasonal timing of LiDAR data collection.

Table 3. Top three regression models from 222 potential models with uncorrelated predictor variables for first-return LiDAR data

Model form	R^2	Error (predicted − observed)		
		Range	Mean	SD
Tree density				
ln(d50) + ln(h80)	0.13	−328.4−269.7	−13.0	111.3
ln(d60) + ln(h80)	0.12	−326.4−272.6	−13.0	111.4
ln(d50) + ln(h90)	0.12	−329.8−272.6	−13.0	111.6
Mean dbh				
ln(d80) + ln(h00) + ln(h100)	0.47	−8.8−6.9	−0.2	3.4
ln(d70) + ln(h00) + ln(h80)	0.46	−9.1−6.5	−0.2	3.4
ln(d70) + ln(h00) + ln(h90)	0.45	−9.2−6.5	−0.2	3.4
Basal area				
ln(h00) + ln(h30)	0.45	−17.5−17.7	−0.5	6.0
ln(d60) + ln(h00) + ln(h70)	0.45	−20.56−15.7	−0.5	6.1
ln(h00) + ln(h20)	0.45	−17.4−18.12	−0.5	6.0
Mean tree height				
ln(h70)	0.53	−4.0−4.8	−0.1	1.9
ln(d90) + ln(h100)	0.52	−4.4−5.0	−0.1	1.9
ln(d80) + ln(h90)	0.52	−4.2−4.9	−0.1	1.9
Lorey's mean tree height				
ln(d90) + ln(h100)	0.62	−4.3−5.9	−0.1	1.9
ln(h70)	0.62	−4.1−5.2	−0.1	1.9
ln(h80)	0.61	−4.3−5.2	−0.1	1.9
Sawtimber volume				
ln(d20) + ln(h60)	0.63	−168.6−152.3	−8.5	57.3
ln(mean) + ln(h00)	0.63	−167.3−128.1	−7.5	57.9
ln(d30) + ln(h60)	0.63	−168.7−156.0	−8.4	57.9
Pulpwood volume				
ln(h00) + ln(h40)	0.64	−268.6−219.0	−7.7	85.9
ln(d20) + ln(h00) + ln(h50)	0.64	−280.5−211.8	−8.2	86.3
ln(d30) + ln(h00) + ln(h50)	0.64	−281.5−217.34	−8.1	86.5

Refer to the Methods for interpretation of predictor variable names. All response variables were log transformed. Data were transformed to original units before the differences between predicted and observed values were calculated.

Previous studies have shown greater variability among LiDAR height measurements for leaf-off conditions than for leaf-on conditions; however, the effect was minimized when only canopy hits (first returns) were used (Næsset 2005). Our LiDAR data were collected in early spring during leaf-off conditions so we built two models, one using all LiDAR returns and a second model using only the first returns. We observed little difference in our results when only the first returns were used. This is in part because the best predictors in both first-return and all-return models tended to be the upper height quantiles and the values of those quantiles were largely determined by the distribution of first-return pulses. Thus, our results confirm the findings of Næsset (2005) and suggest that the general approach of aggregating LiDAR vegetation heights to coarser spatial resolutions before analysis seems to work well regardless of the presence or absence of leaves. In addition, the results for stem volume estimation obtained by Hollaus (2006) were similar when leaf-on and leaf-off data were compared. However, models developed from leaf-off data should not be applied to leaf-on data because the distributions of LiDAR returns in the canopy will almost certainly be different.

Altered footprint size or laser output energy could change the distribution of laser hits in the canopy. With pulse footprints of nearly 60 cm in diameter, we expected that only large objects (tree stems and thick branches) would reflect enough energy to register with the sensor (Goodwin et al. 2006). We found that in our leaf-off conditions, nearly 70% of our pulses were classified as first returns, and we saw little difference in performance between models constructed with all returns compared with those with only first returns. In addition, more than two-thirds of our returns had >0.9 m height, and most of these were reflected from the canopy (Figure 1). We assumed that the remaining one-third of pulses represented the ground surface or noise around the ground surface. Smaller footprints might have produced greater accuracy estimates of within-canopy heights (Andersen et al. 2006). Our LiDAR data had a relatively large footprint, our returns may represent laser reflections from multiple stems and branches at a given height in the canopy, and this effect could have helped to quantify the amount of canopy biomass or volume.

The accuracy and detail of LiDAR-derived elevation models are important when they are used as a baseline for calculating vegetation heights because any errors in the elevation models are propagated to vegetation heights (Reutebuch et al. 2003, Clark et al. 2004, Hopkinson et al. 2005). Errors in elevation models are not always random and are dependent on vegetation and terrain; generally elevation errors are greater in dense vegetation or steep terrain where a smaller number of LiDAR pulses penetrate to the ground (Reutebuch et al. 2003, Hollaus et al. 2006). The estimated error for the LiDAR elevation measurements was 15 cm, and it is unlikely that this error contributed much to the errors in our results. Vegetation height error will also be related to the resolution of the

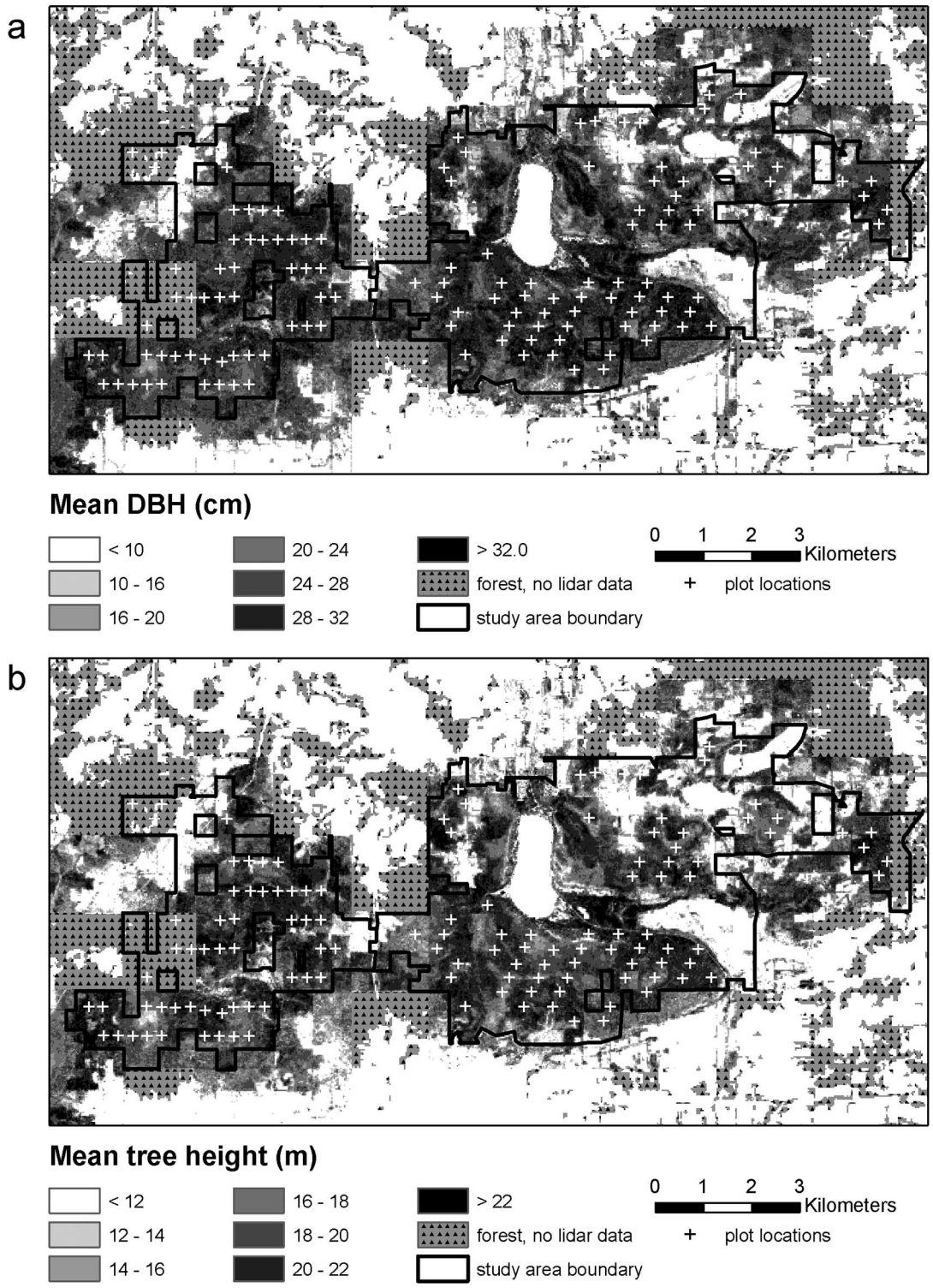

Figure 4. Mapped results for (a) mean dbh and (b) mean tree height from multivariate regression models using all LiDAR pulse returns.

elevation model, especially on steep slopes. The resolution of our elevation model was 4.9 m (16 ft), and we did not account for the effects of slope when we calculated tree heights. Small, within-pixel changes in elevation occur at this resolution, but we did not account for slope effects and believe their impact had a negligible effect on tree heights. Because a minimum number of LiDAR ground returns are required to generate accurate elevation models, one of the primary limitations of low-density LiDAR may be the coarse spatial resolution of resulting elevation models (Magnusson et al. 2007, Gobakken and Næsset 2008).

Conclusions

This study demonstrated that low-density LiDAR data can be successfully used to estimate hardwood forest structure and timber volume over large spatial extents even

though the LiDAR data were originally intended for elevation mapping not for a forest survey. We applied methods of aggregating LiDAR returns to gridded pixels that were originally developed for Scandinavian coniferous forests (Næsset 2004). The success of our results demonstrates that the general approach of relating LiDAR height summary variables to forest structure is robust across different forest types and can be applied to extensive areas using LiDAR data with low pulse densities.

In this study, we did not use any prior information such as stand boundaries or site index measures. This decision was largely due to the lack of existing data. Hence, our field data spanned a greater range of variability than that for many other LiDAR-based studies of forest structure, which stratified sampling across different stands based on site index (Næsset 2002), age and management history (Lim et al. 2003), or species composition (Maclean and Krabill 1986). Even though our regression models left some variability unexplained, they demonstrate the usefulness of LiDAR surveys even when little existing information is incorporated.

LiDAR data are being increasingly collected for a variety of reasons, but LiDAR data collection missions can be expensive. Deriving multiple products from LiDAR data can help to offset the data collection costs. Maps of vegetation and forest structure are essential for land management and conservation planning (Avery and Burkhart 2002, Hyde et al. 2005, Nelson et al. 2005). Broad-scale coverage of vegetation structure is easily produced form LiDAR-based models and could be combined with other spatial data for ecological research, land management, and conservation planning (Figure 4). This study demonstrated that low-density LiDAR data collected for terrain mapping could be useful for such applications.

Literature Cited

ANDERSEN, H.E., S.E. REUTEBUCH, AND R.J. MCGAUGHEY. 2006. A rigorous assessment of tree height measurements obtained using airborne lidar and conventional field methods. *Can. J. Remote Sens*. 32(5):355–366.

ANDERSON, E.S., J.A. THOMPSON, AND R.E. AUSTIN. 2005. LIDAR density and linear interpolator effects on elevation estimates. *Int. J. Remote Sens*. 26(18):3889–3900.

AVERY, T.E., AND H.E. BURKHART. 2002. *Forest measurements*. McGraw-Hill, Boston, MA.

BALTSAVIAS, E.P.1999a. Airborne laser scanning: Basic relations and formulas. *ISPRS J. Photogramm. Remote Sens*. 54(2–3): 199–214.

BALTSAVIAS, E.P.1999a. Airborne laser scanning: Existing systems and firms and other resources. *ISPRS J. Photogramm. Remote Sens*. 54(2–3):164–198.

BLAIR, J.B., D.B. COYLE, J.L. BUFTON, AND D.J. HARDING. 1994. Optimization of an airborne laser altimeter for remote sensing of vegetation and tree canopies. P. 939–941 in *Proceedings of the international geoscience and remote sensing symposium.* IEEE Geoscience and Remote Sensing Society, Piscataway, NJ.

BLAIR, J.B., AND M.A. HOFTON. 1999. Modeling laser altimeter return waveforms over complex vegetation using high-resolution elevation data. *Geophys. Res. Lett*. 26(16):2509–2512.

BLAIR, J.B., D.L. RABINE, AND M.A. HOFTON. 1999. The Laser Vegetation Imaging Sensor: A medium-altitude, digitisation-only, airborne laser altimeter for mapping vegetation and topography. *ISPRS J. Photogramm. Remote Sens*. 54(2–3): 115–122.

BRANDTBERG, T. 2007. Classifying individual tree species under leaf-off and leaf-on conditions using airborne lidar. *ISPRS J. Photogramm. Remote Sens.* 61(5):325–340.

BRANDTBERG, T., AND F. WALTER. 1998. Automated delineation of individual tree crowns in high spatial resolution aerial images by multiple-scale analysis. *Mach. Vis. Applic*. 11(2): 64–73.

BRANDTBERG, T., T.A. WARNER, R.E. LANDENBERGER, AND J.B. MCGRAW. 2003. Detection and analysis of individual leaf-off tree crowns in small footprint, high sampling density lidar data from the eastern deciduous forest in North America. *Remote Sens. Environ*. 85(3):290–303.

BUFTON, J.L., J.B. GARVIN, J.F. CAVANAUGH, L. RAMOSIZQUIERDO, T.D. CLEM, AND W.B. KRABILL. 1991. Airborne lidar for profiling of surface-topography. *Opt. Eng*. 30(1):72–78.

CANHAM, C.D., A.C. FINZI, S.W. PACALA, AND D.H. BURBANK. 1994. Causes and consequences of resource heterogeneity in forests—Interspecific variation in light transmission by canopy trees. *Can. J. For. Res*. 24(2):337–349.

CHEN, J.Q., S.C. SAUNDERS, T.R. CROW, R.J. NAIMAN, K.D. BROSOFSKE, G.D. MROZ, B.L. BROOKSHIRE, AND J.F. FRANKLIN. 1999. Microclimate in forest ecosystem and landscape ecology—Variations in local climate can be used to monitor and compare the effects of different management regimes. *Bioscience* 49(4):288–297.

CLARK, M.L., D.B. CLARK, AND D.A. ROBERTS. 2004. Small-footprint lidar estimation of sub-canopy elevation and tree height in a tropical rain forest landscape. *Remote Sens. Environ*. 91(1):68–89.

COBBY, D.M., D.C. MASON, AND I.J. DAVENPORT. 2001. Image processing of airborne scanning laser altimetry data for improved river flood modelling. *ISPRS J. Photogramm. Remote Sens.* 56(2):121–138.

DONNELLAN, A., P. ROSEN, J. GRAF, A. LOVERRO, A. FREEMAN, R. TREUHAFT, R. OBERTO, M. SIMARD, E. RIGNOT, R. KWOK, X. PI, J.B. BLAIR, W. ABDALATI, J. RANSON, H. ZEBKER, B. HAGER, H. SHUGART, M. FAHNESTOCK, AND R. DUBAYAH. 2008. Deformation, ecosystem structure, and dynamics of ice (DESDynI). P. 1–13 in *2008 IEEE aerospace conference proceedings*. IEEE, New York, NY.

DUBAYAH, R., J.B. BLAIR, J.L. BUFTON, D.B. CLARK, J. JAJA, R.G. KNOX, S.B. LUTHCKE, S. PRINCE, AND J.F. WEISHAMPEL. 1997. The Vegetation Canopy Lidar mission. P. 100–112 in *Land satellite information in the next decade. II: Sources and applications.* American Society for Photogrammetry and Remote Sensing, Bethesda, MD.

EFRON, B. 1982. *The jackknife, the bootstrap and other resampling plans*. Society for Industrial and Applied Mathematics, Philadelphia, PA.

EK, A.R., E.T. BIRDSALL, AND R.J. SPEARS. 1981. *Total and merchantable tree height equations for Lake States tree species*. Staff Paper Ser. No. 27. Minnesota Agricultural Experiment Station, University of Minnesota, St. Paul, MN.

GAVIN, J., J. BUFTON, J. BLAIR, D. HARDING, S. LUTHCKE, J. FRAWLEY, AND D. ROWLANDS. 1998. Observations of the Earth's topography from the Shuttle Laser Altimeter (SLA): Laser-pulse echo-recovery measurements of terrestrial surfaces. *Phys. Chem. Earth* 23:1053–1068.

GEVORKIANTZ, S.R., AND L.P. OLSEN. 1955. *Composite volume tables for timber and their application in the Lake States.* Tech. Bull. 1104. US Department of Agriculture, Washington, DC.

GOBAKKEN, T., AND E. NÆSSET. 2008. Assessing effects of laser point density, ground sampling intensity, and field sample plot size on biophysical stand properties derived from airborne laser scanner data. *Can. J. For. Res*. 38:1095–1109.

GOODWIN, N.R., N.C. COOPS, AND D.S. CULVENOR. 2006. Assessment of forest structure with airborne LiDAR and the effects of platform altitude. *Remote Sens. Environ*. 103(2):140–152.

HAALA, N., AND C. BRENNER.1999. Extraction of buildings and trees in urban environments. *ISPRS J. Photogramm. Remote Sens.* 54(2–3):130–137.

HARDING, D.J., J.B. BLAIR, J.B. GARVIN, AND W.T. LAWRENCE. 1994. Laser altimetry waveform measurements of vegetation canopy structure. P. 1251–1253 in *Proc. of IGARRS '94 conference*, Pasadena, CA. IEEE, New York, NY.

HARDING, D.J., AND C.C. CARABAJAL. 2005. ICES at waveform measurements of within-footprint topographic relief and vegetation vertical structure. *Geophys. Res. Lett*. 32(21):1–4.

HILL, R.A., AND A.G. THOMSON. 2005. Mapping woodland species composition and structure using airborne spectral and LiDAR data. *Int. J. Remote Sens*. 26(17):3763–3779.

HINSLEY, S.A., R.A. HILL, D.L.A. GAVEAU, AND P.E. BELLAMY. 2002. Quantifying woodland structure and habitat quality for birds using airborne laser scanning. *Funct. Ecol*. 16(6): 851–857.

HOLLAUS, M. 2006. *Large scale applications of airborne laser scanning for a complex mountainous environment.* Technishe Universität Wein, Wein, Austria. 127 p.

HOLLAUS, M., W. WAGNER, C. EBERHOFER, AND W. KAREL. 2006. Accuracy of large-scale canopy heights derived from LiDAR data under operational constraints in a complex alpine environment. *ISPRS J. Photogramm. Remote Sens.* 60(5):323–338.

HOLMGREN, J. 2004. Prediction of tree height, basal area and stem volume in forest stands using airborne laser scanning. *Scand. J. For. Res*. 19(6):543–553.

HOPKINSON, C., L.E. CHASMER, G. SASS, I.F. CREED, M. SITAR, W. KALBFLEISCH, AND P. TREITZ. 2005. Vegetation class dependent errors in lidar ground elevation and canopy height estimates in a boreal wetland environment. *Can. J. Remote Sens*. 31(2):191–206.

HUDAK, A.T., M.A. LEFSKY, W.B. COHEN, AND M. BERTERRETCHE. 2002 Integration of lidar and Landsat ETM plus data for estimating and mapping forest canopy height. *Remote Sens. Environ*. 82(2–3):397–416, 2002.

HYDE, P., R. DUBAYAH, B. PETERSON, J.B. BLAIR, M. HOFTON, C. HUNSAKER, R. KNOX, AND W. WALKER. 2005. Mapping forest structure for wildlife habitat analysis using waveform lidar: Validation of montane ecosystems. *Remote Sens. Environ*. 96(3–4):427–437.

HYYPPÄ, J., O. KELLE, M. LEHIKOINEN, AND M. INKINEN. 2001. A segmentation-based method to retrieve stem volume estimates from 3-D tree height models produced by laser scanners. *IEEE Trans. Geosci. Remote Sens*. 39(5):969–975.

JAKUBAUSKAS, M.E., K.P. LULLA, AND P.W. MAUSEL. 1990. Assessment of vegetation change in a fire-altered forest landscape. *Photogramm. Eng. Remote Sens*. 56(3):371–377.

KUCHARIK, C.J., J.M. NORMAN, AND S.T. GOWER. 1999. Characterization of radiation regimes in nonrandom forest canopies: Theory, measurements, and a simplified modeling approach. *Tree Physiol*. 19(11):695–706.

LECKIE, D., F. GOUGEON, D. HILL, R. QUINN, L. ARMSTRONG, AND R. SHREENAN. 2003a. Combined high-density lidar and multispectral imagery for individual tree crown analysis. *Can. J. Remote Sens*. 29(5):633–649.

LECKIE, D.G., F.A. GOUGEON, N. WALSWORTH, AND D. PARADINE. 2003b. Stand delineation and composition estimation using semi-automated individual tree crown analysis. *Remote Sens. Environ*. 85(3):355–369.

LEFSKY, M.A., W.B. COHEN, S.A. ACKER, G.G. PARKER, T.A. SPIES, AND D. HARDING. 1999. Lidar remote sensing of the canopy structure and biophysical properties of Douglas-fir western hemlock forests. *Remote Sens. Environ*. 70(3): 339–361.

LEFSKY, M.A., W.B. COHEN, G.G. PARKER, AND D.J. HARDING. 2002. Lidar remote sensing for ecosystem studies. *Bioscience* 52(1):19–30.

LIM, K., P. TREITZ, K. BALDWIN, I. MORRISON, AND J. GREEN. 2003. Lidar remote sensing of biophysical properties of tolerant northern hardwood forests. *Can. J. Remote Sens*. 29(5): 658–678.

LOHR, U. 1998. Digital elevation models by laser scanning. *Photogramm. Rec*. 16(91):105–109.

MAAS, H.G., AND G. VOSSELMAN. 1999. Two algorithms for extracting building models from raw laser altimetry data. *ISPRS J. Photogramm. Remote Sens.* 54(2–3):153–163.

MACARTHUR, R.H., AND J.W. MACARTHUR. 1969. On bird species diversity. *Ecology* 42:594–598.

MACLEAN, G.A., AND W.B. KRABILL. 1986. Gross-merchantable timber volume estimation using an airborne lidar system. *Can. J. Remote Sens*. 12(1):7–18.

MAGNUSSON, M., J.E.S. FRANSSON, AND J. HOLMGREN. 2007. Effects on estimation accuracy of forest variables using different pulse density of laser data. *For. Sci*. 53(6):619–626.

MALTAMO, M., P. PACKALEN, J. PEUHKURINEN, A. SUVANTO, A. PESONEN, AND J. HYYPPA. 2007. Experiences and possibilities of ALS based forest inventory in Finland. P. 270–279 in *IAPRS workshop on laser scanning 2007 and SilviLaser 2007*, Espoo, Finland.

MALTAMO, M., P. PACKALEN, X. YU, K. EERIKAINEN, J. HYYPPA, AND J. PITKANEN. 2005. Identifying and quantifying structural characteristics of heterogeneous boreal forests using laser scanner data. *For. Ecol. Manag*. 216(1–3):41–50.

MCCOMBS, J.W., S.D. ROBERTS, AND D.L. EVANS. 2003. Influence of fusing lidar and multispectral imagery on remotely sensed estimates of stand density and mean tree height in a managed loblolly pine plantation. *For. Sci*. 49(3):457–466.

NÆSSET, E. 1997a. Determination of mean tree height of forest stands using airborne laser scanner data. *ISPRS J. Photogramm. Remote Sens.* 52(2):49–56.

NÆSSET, E. 1997b. Estimating timber volume of forest stands using airborne laser scanner data. *Remote Sens. Environ*. 61(2): 246–253.

NÆSSET, E. 2002. Predicting forest stand characteristics with airborne scanning laser using a practical two-stage procedure and field data. *Remote Sens. Environ*. 80(1):88–99.

NÆSSET, E. 2004. Practical large-scale forest stand inventory using a small-footprint airborne scanning laser. *Scand. J. For. Res*. 19(2):164–179.

NÆSSET, E. 2005. Assessing sensor effects and effects of leaf-off and leaf-on canopy conditions on biophysical stand properties derived from small-footprint airborne laser data. *Remote Sens. Environ*. 98(2–3):356–370.

NÆSSET, E., T. GOBAKKEN, J. HOLMGREN, H. HYYPPÄ, J. HYYPPÄ, M. MALTAMO, M. NILSSON, H. OLSSON, A. PERSSON, AND U. SÖDERMAN. 2004. Laser scanning of forest resources: The Nordic experience. *Scand. J. For. Res*. 19(6):482–499.

NELSON, R., C. KELLER, AND M. RATNASWAMY. 2005. Locating and estimating the extent of Delmarva fox squirrel habitat using an airborne LiDAR profiler. *Remote Sens. Environ*. 96(3–4):292–301.

NELSON, R., W. KRABILL, AND G. MACLEAN. 1984. Determining

forest canopy characteristics using airborne laser data. *Remote Sens. Environ*. 15(3):201–212.

NELSON, R., W. KRABILL, AND J. TONELLI. 1988. Estimating forest biomass and volume using airborne laser data. *Remote Sens. Environ*. 24(2):247–267.

NI-MEISTER, W., D.L.B. JUPP, AND R. DUBAYAH. 2001. Modeling lidar waveforms in heterogeneous and discrete canopies. *IEEE Trans. Geosci. Remote Sens*. 39(9):1943–1958.

NILSSON, M. 1996. Estimation of tree weights and stand volume using an airborne lidar system. *Remote Sens. Environ*. 56(1):1–7.

OLDEN, J.D., AND D.A. JACKSON. 2000. Torturing data for the sake of generality: How valid are our regression models? *Ecoscience* 7(4):501–510.

PINHERIO, J.C., AND D.M. BATES. 2002. *Mixed-effects models in S and S-PLUS*. Springer, New York, NY.

POPESCU, S.C., R.H. WYNNE, AND J.A. SCRIVANI. 2004. Fusion of small-footprint lidar and multispectral data to estimate plot-level volume and biomass in deciduous and pine forests in Virginia, USA. *For. Sci*. 50(4):551–565.

R DEVELOPMENT CORE TEAM. 2007. *R: A language for computing*. R Foundation for Statistical Computing, Vienna, Austria.

RADELOFF, V.C., D.J. MLADENOFF, AND M.S. BOYCE. 1999. Detecting jack pine budworm defoliation using spectral mixture analysis: Separating effects from determinants. *Remote Sens. Environ*. 69(2):156–169.

REUTEBUCH, S.E., R.J. MCGAUGHEY, H.E. ANDERSEN, AND W.W. CARSON. 2003. Accuracy of a high-resolution lidar terrain model under a conifer forest canopy. *Can. J. Remote Sens*. 29(5):527–535.

RIANO, D., E. MEIER, B. ALLGOWER, E. CHUVIECO, AND S.L. USTIN. 2003. Modeling airborne laser scanning data for the spatial generation of critical forest parameters in fire behavior modeling. *Remote Sens. Environ*. 86(2):177–186.

SINGER, M.T., AND C.G. LORIMER. 1997. Crown release as a potential old-growth restoration approach in northern hardwoods. *Can. J. For. Res*. 27(8):1222–1232.

STONE, M. 1974. Cross-validatory choice and assessment of statistical predictions. *J. R. Stat. Soc. Ser. B Methodol*. 36(2): 111–147.

SUN, G.Q., AND K.J. RANSON. 2000. Modeling lidar returns from forest canopies. *IEEE Trans. Geosci. Remote Sens*. 38(6):2617–2626.

TAKAHASHI, T., K. YAMAMOTO, Y. SENDA, AND M. TSUZUKU. 2005. Estimating individual tree heights of sugi (*Cryptomeria japonica* D. Don) plantations in mountainous areas using small-footprint airborne LiDAR. *J. For. Res*. 10(2):135–142.

US FOREST SERVICE. 2006. *National Volume Estimator Library (NVEL)—Library of national tree volume estimators*. US Forest Service, Washington DC.

VAN AARDT, J.A.N., R.H. WYNNE, AND R.G. ODERWALD. 2006. Forest volume and biomass estimation using small-footprint lidar-distributional parameters on a per-segment basis. *For. Sci*. 52(6):636–649.

WARING, R.H. 1983. Estimating forest growth and efficiency in relation to canopy leaf-area. *Adv. Ecol. Res*. 13:327–354.

WING, M.G., D. SOLMIE, AND L. KELLOGG. 2004. Comparing digital range finders for forestry applications. *J. For*. 102(4):16–20.

WOLTER, P.T., D.J. MLADENOFF, G.E. HOST, AND T.R. CROW. 1995. Improved forest classification in the northern Lake-States using multitemporal Landsat imagery. *Photogramm. Eng. Remote Sens*. 61(9):1129–1143.

WULDER, M.A., AND S.E. FRANKLIN. 2003. *Remote sensing of forest environments: Concepts and case studies*. Kluwer Academic Publishers, Boston, MA. 552 p.